

TTK is a potential regulator of tumor progression correlated with dedifferentiation and immune cell infiltration in papillary thyroid cancer

Jun-Jie Ma¹, Cheng Xiang¹, Jian-Wei Wang²

¹Department of Thyroid Surgery, The Second Affiliated Hospital of Zhejiang University School of Medicine, Hangzhou 310009, Zhejiang, China

²The Colorectal Surgery, The Second Affiliated Hospital of Zhejiang University School of Medicine, Hangzhou 310009, Zhejiang, China

Correspondence to: Jian-Wei Wang; email: sypzju@zju.edu.cn

Keywords: TTK, papillary thyroid cancer, tumorigenesis, prognosis, biomarker

Received: May 12, 2023

Accepted: September 9, 2023

Published: October 6, 2023

Copyright: © 2023 Ma et al. This is an open access article distributed under the terms of the [Creative Commons Attribution License](https://creativecommons.org/licenses/by/3.0/) (CC BY 3.0), which permits unrestricted use, distribution, and reproduction in any medium, provided the original author and source are credited.

ABSTRACT

Objective: To investigate the role and clinical significance of threonine tyrosine kinase (TTK) in papillary thyroid cancer (PTC).

Methods: TTK expression in PTC and normal groups were compared using TCGA data and *in vitro* experiments. The prognostic value of TTK and its possible role in PTC dedifferentiation was evaluated. Next, TTK involvement in PTC occurrence and progression was analyzed via *in vitro* experiments. Subsequently, analyses of enrichment and immune cell infiltration were conducted to reveal the possible mechanism. Finally, we predicted the target miRNAs followed by performing a luciferase reporter experiment.

Results: TTK upregulation was observed in PTC, and its elevated level was significantly related to an unfavorable prognosis ($P < 0.05$). Interestingly, TTK negatively correlated with thyroid differentiation score (TDS), and patients with higher TDS showed longer survival (all $P < 0.05$). PTC cell growth, migration, and invasion were inhibited upon TTK knockdown. Besides, TTK was involved in metabolic processes and regulated cell adhesion molecules pathway. Its overexpression was positively associated with immune cell infiltrates ($P < 0.05$). Moreover, miR-582-5p was an upstream target of TTK.

Conclusion: TTK serves as a potential biomarker for tumorigenesis and prognosis in PTC, especially for those that may differentiate into more aggressive thyroid cancers.

INTRODUCTION

Thyroid cancer (THCA) is the most prevalent malignancy of the endocrine system, of which morbidity has been increasing worldwide [1]. Its incidence ranked 9th leading cancer among malignancies globally in 2020 [2, 3]. Papillary thyroid cancer (PTC) accounts for 80–90% of all THCA cases and tends to metastasize to the cervical lymph nodes [4, 5]. Fine-needle aspiration cytology is a gold standard diagnosis of PTC; however, the rate of indeterminate

lesions offers a challenge in clinical management [6, 7]. Although the vast majority of patients with PTC have a favorable 5-year survival rate of over 95% after standard surgery, radioactive iodine therapy, and thyroid-stimulating hormone suppression therapy, 5–10% of them still experience recurrence or distant metastasis since some PTC dedifferentiate into more aggressive phenotypes [8, 9]. Multiple factors contribute to the initiation and development of PTC, including epigenetic alterations, environmental exposures, and genetic mutations [10]. Epigenetic alterations include

Linc00941, MiR21, and MiR146b and genetic mutations include the driver point mutations of RAS and BRAF [11, 12]. Some of these markers have been used in the clinic as diagnostic markers and therapeutic targets for recurrence and metastasis, but there are still significant limitations in diagnostic efficiency and treatment side effects [13]. Therefore, it is necessary for robust molecular biomarkers to be developed for improving the diagnosis and treatment management of PTC.

Threonine tyrosine kinase (TTK) also known as Mps1, is a dual-specificity kinase that phosphorylates tyrosine as well as serine/threonine [14]. In addition to promoting mitotic checkpoint complex formation, TTK regulates cytokinesis, responds to DNA damage, and facilitates proper chromosome alignment [15]. As a mediator of the spindle assembly checkpoint (SAC), TTK delays anaphase until all chromosomes are properly attached to the mitotic spindle, which ensures accurate chromosomal segregation and preserves genomic integrity [16]. Since most cancer cells are aneuploidy, they rely heavily on SACs to adequately segregate their abnormal karyotypes during mitosis [17]. Thus, TTK promotes cancer cell proliferation and invasion, and its upregulation leads to poor prognosis for various cancers of the breast, colon, and glioblastoma [17–19]. However, the impact of TTK on PTC progression and its underlying mechanism remains to be clarified.

Herein, we used efficient bioinformatics tools to analyze the TTK expression and validated it in PTC and normal thyroid cells. After examining the clinical value, we assessed its influence on cancer cell proliferation, apoptosis, cell cycle, invasion, and migration. Then, the biological processes and gene set enrichment analysis (GSEA) was conducted to explore the potential regulatory pathway of TTK, which was validated using *in vitro* experiments. Immune cell infiltration analysis was performed using the TCGA data. Finally, the upstream miRNAs were predicted to further determine the fundamental mechanism.

MATERIALS AND METHODS

TTK expression analysis

TIMER (<https://cistrome.shinyapps.io/timer/>) was employed to analyze differential TTK expression in pan-cancer in the “Diff Exp” column. Then, UCSC Xena (<https://xenabrowser.net/>) was searched to extract the expression and clinical data of TCGA-THCA. PTC samples exhibiting complete expression data matched with survival information were included. Unpaired and paired *t*-tests were used for analyzing TTK expression in PTC and normal groups.

Besides, all participants were assigned to low (TTK-L) and high expression groups (TTK-H) by the median TTK level. The correlation of TTK expression as a categorical variable and the clinical factors was evaluated using the chi-square test, and univariate logistic regression analysis. As a continuous variable, the correlation with these parameters was analyzed by the Student’s *t*-test or one-way ANOVA.

Clinical significance of TTK in PTC

Firstly, the receiver operating characteristic (ROC) curves were drawn to determine the diagnostic value of TTK in PTC. Next, the effect of TTK on clinical outcomes was analyzed by the Kaplan-Meier plotter method. Disease-free interval (DFI) refers to the measure of time after treatment during which no regional recurrence/distant metastasis is found [20]. Disease-specific survival (DSS) refers to the percentage of people who died from a specific disease in a defined period [21]. Overall survival (OS) is defined as the time from the operation to death from any cause [22]. Progression-free interval (PFI) was measured from the date of initial treatment randomization to the time of disease recurrence [23].

Following this, its predictive value for survival status was evaluated using the R package “timeROC”. The Cox regression analyses were conducted to obtain the independent risk factors for PTC. Finally, nomogram models were constructed and the calibration curves were plotted.

Subsequently, the association of TTK expression with thyroid differentiation score (TDS) was assessed using the Pearson correlation test to explore the value of TTK in PTC dedifferentiation. The mRNA expression level of 16 thyroid-specific genes was used to calculate the TDS. Then, a median TDS level was used to divide the patients into high- and low-TDS groups. The correlation of TDS with DFI and PFI was assessed by the Kaplan-Meier plotter method.

Cell lines and cell culture

Normal thyroid cell line Nthy-ori 3–1 and PTC cell lines TPC1 and BCPAP were used in this study (Shanghai, China). The cells were cultured in Dulbecco’s modified Eagle’s medium (Gibco, Waltham, MA, USA) supplemented with 10% fetal bovine serum and 100 units/ml of penicillin-streptomycin (Gibco, USA) at 37°C in a humidified atmosphere of 5% CO₂.

Quantitative real-time PCR (qRT-PCR)

Total RNA was isolated from cells using TRIzol reagent (Invitrogen, Carlsbad, CA, USA). The supernatant was

Table 1. Primer sequences.

Name	Primer sequences
Human TTK forward	5'-CCGAGATTTGGTTGTGCCTGGA-3'
Human TTK reverse	5'-CATTCGACACCAGAGGTTCCCTTG-3'
Human miR-582-5p forward	5'-GCACACATTGAAGAGGACAGAC-3'
Human miR-582-5p reverse	5'-TATTGAAGGGGGTTCTGGTG-3'
Human GAPDH forward	5'-GAAGGTGAAGGTCGGAGTC-3'
Human GAPDH reverse	5'-GAAGATGGTGATGGGATTTC-3'

transferred after centrifugation at 12 000 g at 4°C for 10 min and was placed at room temperature for 5 min, added with 0.2 ml chloroform, vibrated for 15 s, and placed at 37°C for 2–3 min. After the water phase was transferred and the supernatant removed, the RNA was stored at –70°C. Following reverse transcription, qRT-PCR was performed on an Mx3000P system (Agilent Stratagene). GAPDH was utilized as an internal control. Relative expressions of TTK and miR-582-5p were measured using the $2^{-\Delta\Delta Ct}$ method. The primer sequences are shown in Table 1.

Western blotting

Cells were lysed with RIPA lysis buffer (Beyotime, Shanghai, China) and the protein concentration was quantified by the BCA method. Then, the proteins were dissolved by sodium dodecyl sulfate-polyacrylamide gel electrophoresis and were transferred to polyvinylidene fluoride (PVDF) membranes (Beyotime, Shanghai, China), blocked with 5% skimmed milk. The membranes were incubated with the following primary antibodies at 4°C overnight: anti-TTK (Abcam), anti-GAPDH (Abcam), anti-Bcl2 (Abcam), anti-Bax (Abcam), anti-CDK2 (Abcam), anti-Cyclin D1 (Abcam), anti-p21 (Abcam), anti-E-cadherin (Abcam), anti-N-cadherin (Abcam), anti-Vimentin (Abcam), anti-MMP2 (Abcam), anti-Snail (Abcam), anti-Twist1 (Abcam), anti-ICAM1 (Abcam), anti-VCAM1 (Abcam), anti-MMP9 (Abcam). The next day, after incubation with a goat anti-rabbit IgG secondary antibody (Abcam), the PVDF membrane was subjected to chemiluminescence detection by an ECL western blotting detection kit (Servicebio, Wuhan, China).

Cell transfection

Eukaryotic expression vectors encoding TTK and plasmids encoding shRNAs against TTK were synthesized by GenePharma (Shanghai, China). Next, the PTC cells were transfected with shRNA plasmids according to the manufacturer's instructions. The transduced cells were selected with 2 µg/mL puromycin for 4 weeks. Lentiviral particles packaging the shRNA are targeting TTK #1 (5'-AATGAACAAAGTGAGA

GACAT-3'), TTK #2 (5'-UGAACAAAGUGAGAGA CAUTT-3'), TTK #3 (5'-GGAUUUAAGUGGCAGA GAGAATT-3'), and the scramble control (5'-TTC TCCGAACGTGTACGT-3').

CCK8 and colony formation assays

CCK8 assay was utilized to monitor cell growth by the manufacturer's protocols. Cells were seeded in 96-well plates (5×10^3 cells/well) and CCK8 solution (10 µL) was added to each well. Next, a microplate reader was used to measure the absorbance at 450 nm after incubation of the cells at 37°C for 2 h. Colony formation assay was conducted for verifying how TTK affects PTC cell proliferation. PTC cells transfected with shRNA plasmids were seeded into well of 6-well plates and cultured for 2–3 weeks until colony formation; fresh media was provided every 3 days. Finally, to fix the colonies with paraformaldehyde (1 ml/well), stain them with crystal violet solution (1 ml/well), and quantify them.

Flow cytometry assay

Flow cytometry assay was conducted as previously described [24]. Firstly, cells were resuspended in binding buffer (300 µL) after being washed twice, and then Annexin V-FITC solution (5 µL) was added for incubation in the dark for 15 min. Following propidium iodide (PI) (10 µL) supplementation and culture for 30 min, the apoptotic cells were evaluated by an Annexin V-FITC/PI Apoptosis Detection kit (BD Biosciences, Franklin Lakes, NJ, USA). Additionally, the PTC cells during the exponential growth phase were harvested, and single-cell suspensions containing 1×10^5 cells were fixed with 70% alcohol. Then, the cell cycle analysis was performed with a FACScan flow cytometer, and the data were analyzed using FlowJo software.

Transwell assay

Transwell assay was utilized to evaluate the invasive capacity of the cells. The cells in the logarithmic growth phase were trypsinized, resuspended in a serum-free

medium, and adjusted to a density of 1×10^6 cells/mL. Cell suspension (200 μ L) and 600 μ L medium were added to the top and bottom compartments, respectively, and then the cells were cultured at room temperature for 24 h. Following this, cells migrating to the bottom surface were fixed with methanol and dyed with 0.1% crystal violet at 37°C in the dark for 30 min. After rinsing the stained cells with PBS three times, they were observed through a light microscope.

Wound-healing assay

We seeded the cells into 6-well plates (5×10^5 cells/well). When the cells reached 90% confluence, a sterile 200- μ L pipet tip was used to produce a wound line in the center of the cell monolayer. We took the wound images and recorded the width at 0 h after rinsing two times with PBS. The image of the same location was obtained after 24 h. The cellular migration ability was assessed by measuring changes in scratch space distance.

Enrichment analysis

We first identified differentially expressed genes (DEGs) by the median TTK expression using the “limma” package. The thresholds were set as follows: $P < 0.05$ and $|\log_2(\text{Fold Change})| > 1$. Then, the biological processes of these significant DEGs were analyzed by the “ClusterProfiler” package.

Subsequently, GSEA was performed using the TCGA data. By setting the median as the cutoff value, patients were divided into TTK-H and TTK-L. The number of gene set permutations was 1000 times and a phenotypic label was set as high expression versus low expression.

Immune cell infiltration analysis

Tumor-infiltrating immune cells play an essential role in tumor occurrence, progression, and metastasis. Thus, the immune score and stromal score were calculated using the ESTIMATE algorithm [25]. Besides, the TIMER and xCELL algorithms were adopted to evaluate the expression correlation of TTK with several immune cells.

Luciferase reporter experiment

We predicted the target miRNAs of TTK through DIANA (<http://diana.imis.athena-innovation.gr/DianaTools/index.php>), miRDB (<http://www.mirdb.org/>), and Targetscan (http://www.targetscan.org/vert_72/) databases. The Venn analysis identified nine consistent miRNAs among the three databases and miR-582-5p of interest was selected for further luciferase reporter

experiment [26]. Then, the binding sequence was acquired by the bioinformatics tools, and PCR was implemented to amplify the binding site. The TTK 3'UTR wild-type and mutant plasmids were constructed followed by co-transfecting the recombinant plasmids into TPC1 and BCPAP cells with miR-NC and miR-582-5p mimics, respectively. A dual-luciferase reporter gene assay system was used for luciferase activity determination after 48 h.

Statistical analysis

Data analyses were conducted by GraphPad Prism software (version 8.0.2, San Diego, CA, USA), SPSS software (version 23.0), and R software. Data from the cellular experiments were presented as mean \pm standard deviation. Student's *t*-test was used for two-group comparison, while a one-way ANOVA was adopted to determine the differences for at least three groups. All experiments were repeated at least three times and $P < 0.05$ was defined as statistically significant.

RESULTS

TTK is overexpressed in PTC

TTK transcriptional levels in various cancers were exhibited in Figure 1A. Of note, higher TTK expression was found in PTC in contrast with the normal group (all $P < 0.05$) (Figure 1B, 1C). Moreover, its mRNA level in the PTC cell was significantly higher in contrast with the normal cell, while the BCPAP cell had a notably higher level than the TPC1 cell ($P < 0.05$) (Figure 1D). Besides, we observed the elevated TTK protein level of PTC cells compared with the normal cell (Figure 1E). These results indicated that TTK was upregulated in PTC.

After that, we examined that TTK was remarkably linked to the N stage and histological subtype but was not connected with age and gender (Tables 2, 3). Notably, TTK expression was elevated in the N1 stage; and its expression was upregulated in the PTC-tall cell subtype, followed by PTC-classical and PTC-follicular ($P < 0.05$) (Figure 1F, 1G).

TTK overexpression is related to unfavorable prognosis

The ROC curve was plotted to investigate the significance of TTK in discriminating PTC and normal thyroid tissue with an area under the curve of 0.73 (Figure 2A). In addition, TTK upregulation was closely connected with shorter DFI and PFI ($P < 0.05$) but had no significant association with DSS and OS ($P > 0.05$) (Figure 2B–2E). Moreover, TTK had a certain ability in predicting DFI and PFI status (Figure 2F, 2G).

To reveal the independent prognostic role of TTK, we performed the Cox regression analysis of DFI and PFI. In the univariate analysis, N stage and TTK were significantly related to DFI. The significant factors were then enrolled for multivariate analysis and they remained independent predictors ($P < 0.05$). Moreover,

age, N stage, and TTK could independently predict the PFI ($P < 0.05$) (Table 4). Among these independent predictors, TTK contributed most to predicting the DFI and PFI probability of 3 and 5 years (Figure 3A, 3B). The calibration curves showed good agreement between the prediction by the nomogram and actual observations

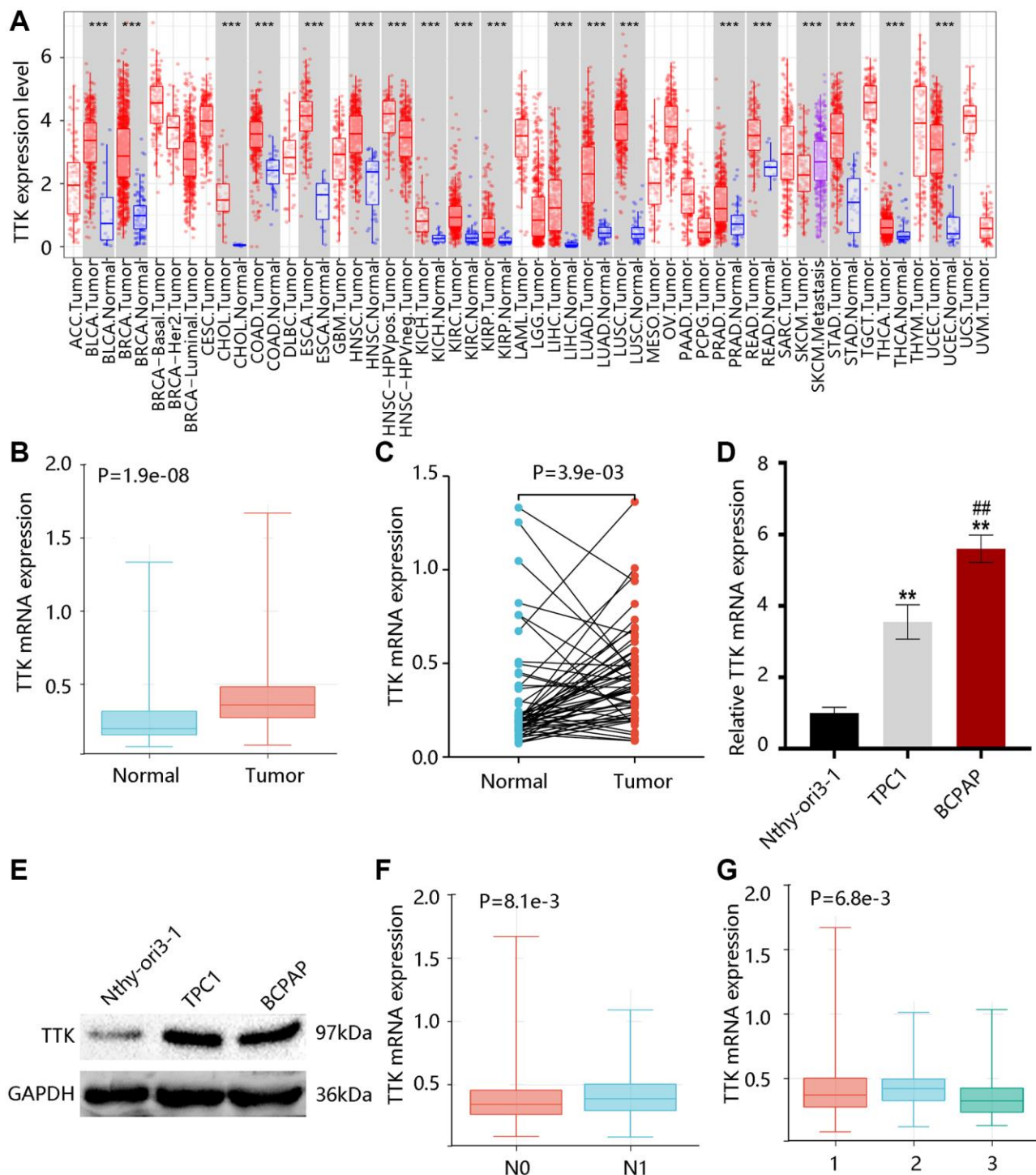


Figure 1. TTK expression profile in papillary thyroid cancer (PTC). (A) TTK expression in pan-cancer. The elevated TTK mRNA level in PTC by the (B) unpaired and (C) paired *t*-tests using TCGA data. Higher TTK (D) mRNA and (E) protein expression in PTC cells. Relationship between TTK and (F) N stage, as well as (G) histological subtype. 1: PTC-classical; 2: PTC-tall cell; 3: PTC-follicular.

Table 2. The correlation between TTK expression and clinicopathological parameters in PTC.

Parameters	Total <i>n</i> (%)	Low TTK <i>n</i> (%)	High TTK <i>n</i> (%)	<i>P</i> -value
Age				
<55	337 (67.1)	171 (68.1)	166 (66.1)	0.635
≥55	165 (32.9)	80 (31.9)	85 (33.9)	
Gender				
Female	366 (72.9)	180 (71.7)	186 (74.1)	0.547
Male	136 (27.1)	71 (28.3)	65 (25.9)	
N stage				
N0	225 (44.8)	125 (49.8)	100 (39.8)	0.013
N1	228 (45.4)	100 (39.8)	128 (51.0)	
Unknown	49 (9.8)	26 (10.4)	23 (9.2)	
Subtype				
PTC-classical	361 (71.9)	174 (69.3)	187 (74.5)	0.010
PTC-tall cell	37 (7.4)	13 (5.2)	24 (9.6)	
PTC-follicular	104 (20.7)	64 (25.5)	40 (15.9)	

Abbreviation: PTC: papillary thyroid cancer.

Table 3. The connection of TTK with clinical factors through univariate logistic regression analysis.

Characteristics	Odds ratio (95% CI)	<i>P</i> -value
Age	0.995 (0.984–1.006)	0.374
Gender	0.886 (0.597–1.314)	0.547
N stage	1.600 (1.104–2.318)	0.013
Subtype	0.800 (0.644–0.993)	0.043

Abbreviation: 95% CI: 95% confidence interval.

(Figure 3C, 3D). These findings implied TTK as a potent prognostic predictor.

TTK negatively correlates with TDS

To examine the potential role of TTK in PTC dedifferentiation, we analyzed the correlation of TTK expression with TDS. TTK was negatively correlated with the expression of 16 thyroid-specific genes (Figure 4A). TTK had a negative correlation with TDS, and patients in the TTK-H presented markedly lower TDS (all $P < 0.05$) (Figure 4B, 4C). Interestingly, high TDS was significantly related to favorable DFI and PFI (all $P < 0.05$) (Figure 4D, 4E). These results suggested that TTK might affect patient prognosis by influencing PTC dedifferentiation.

TTK promotes PTC cell growth

The TTK overexpression and its clinical value in PTC promoted us to investigate its oncogenic effect in PTC. TTK was knocked down in TPC1 and BCPAP cells using TTK-targeting shRNA vectors. We selected shRNA-1 for all following experiments due to its

highest knockdown efficiency as determined by the qRT-PCR and western blotting results (Figure 5A–5D). The TTK-knockdown TPC1 and BCPAP cells significantly suppressed cell proliferation as exhibited by CCK-8 (Figure 5E). Consistent findings were observed in the colony formation assay (Figure 5F). These data indicated that TTK might accelerate PTC cell growth.

TTK promotes PTC cell growth by inhibiting apoptosis and facilitating cell cycle progression

To explore the mechanism of TTK regulating PTC cell growth, we performed analyses of cell apoptosis and cell cycle progression. TTK Knockdown increased TPC1 and BCPAP cell apoptosis (Figure 6A, 6B). Besides, the TTK-knockdown in two PTC cells significantly reduced G1-phase cells, while increasing S-phase and G2-phase cells compared to the control group (Figure 6C, 6D). Decreased Bcl2 protein expression but increased Bax protein expression further confirmed the apoptosis suppression by TTK (Figure 6E). Moreover, the expression of cell cycle-related proteins CDK2 and Cyclin D1 were

downregulated and p21 was upregulated in TTK-knockdown TPC1 and BCPAP cells (Figure 6F). These results revealed that TTK might promote PTC cell growth by suppressing apoptosis and facilitating cell cycle progression.

TTK contributes to cellular invasion and migration

To investigate the effect of TTK in PTC metastasis, we carried out transwell and wound-healing assays. As shown in Figure 7A, the invasive capacity of PTC cells

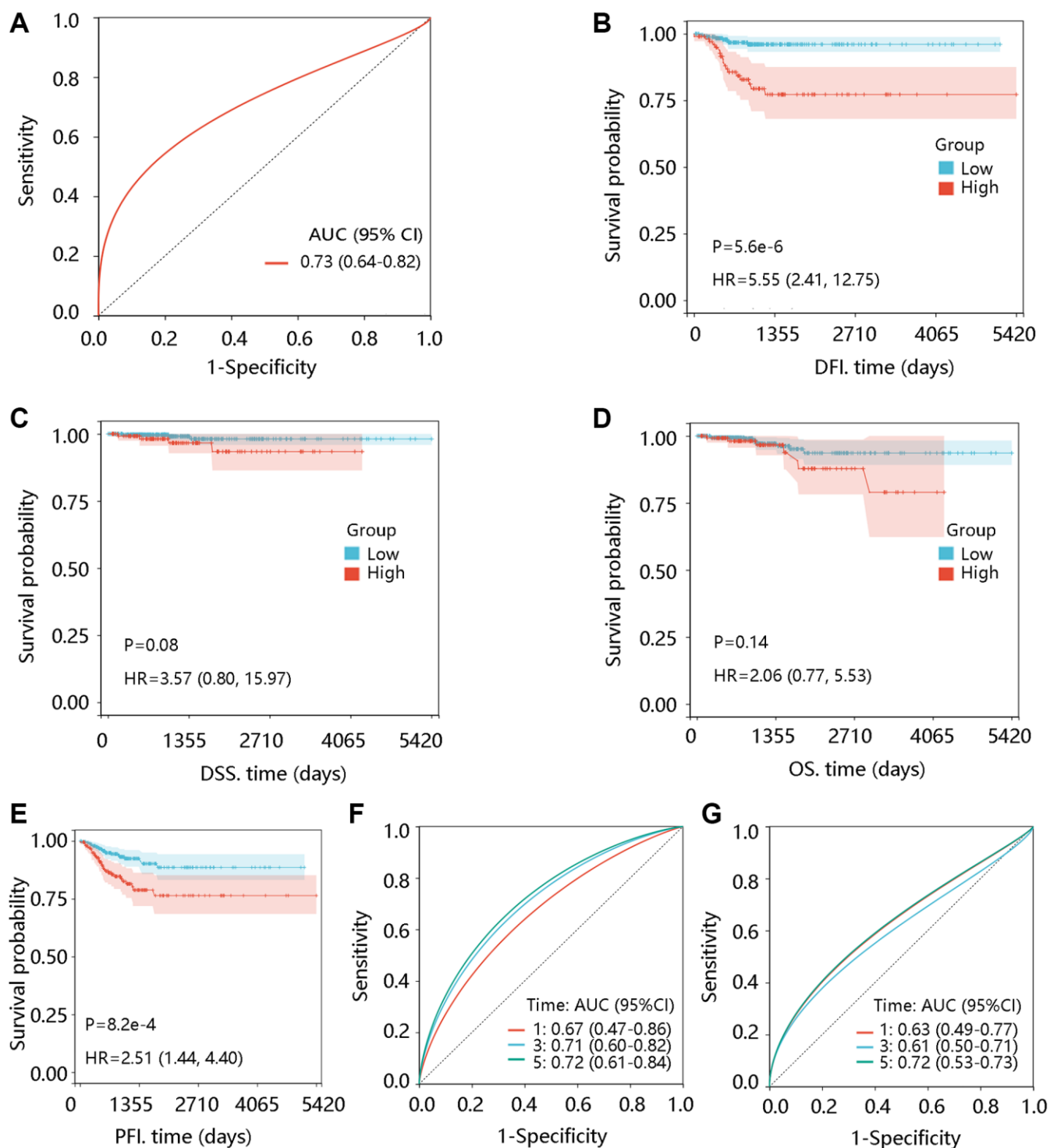


Figure 2. Prognostic significance of TTK in PTC. (A) Value of TTK in distinguishing the PTC and normal tissues. The association of TTK with (B) disease-free interval (DFI), (C) disease-specific survival (DSS), (D) overall survival (OS), and (E) progression-free interval (PFI). TTK showed a certain ability in predicting the (F) DFI and (G) PFI status. Abbreviations: AUC: area under the curve; HR: hazards ratio; 95% CI: 95% confidence interval.

Table 4. Cox regression analysis of TTK and clinical factors for disease-free interval and progression-free interval.

Characteristics	Univariate analysis		Multivariate analysis	
	HR (95% CI)	P value	HR (95% CI)	P-value
Disease-free interval				
Age	0.992 (0.968–1.018)	0.552	/	/
Gender	1.286 (0.540–3.060)	0.570	/	/
N stage	3.090 (1.271–7.513)	0.013	3.381 (1.360–8.405)	0.009
Subtype	0.728 (0.417–1.273)	0.266	/	/
TTK	15.399 (5.421–43.745)	<0.001	19.488 (5.598–67.846)	<0.001
Progression-free interval				
Age	1.019 (1.003–1.036)	0.024	1.020 (1.003–1.037)	0.018
Gender	1.660 (0.943–2.920)	0.079	/	/
N stage	1.850 (1.024–3.343)	0.042	1.926 (1.063–3.490)	0.031
Subtype	0.781 (0.530–1.152)	0.213	/	/
TTK	8.449 (3.263–21.876)	<0.001	6.084 (2.173–17.031)	0.001

Abbreviations: HR: hazard ratio; 95% CI: 95% confidence interval.

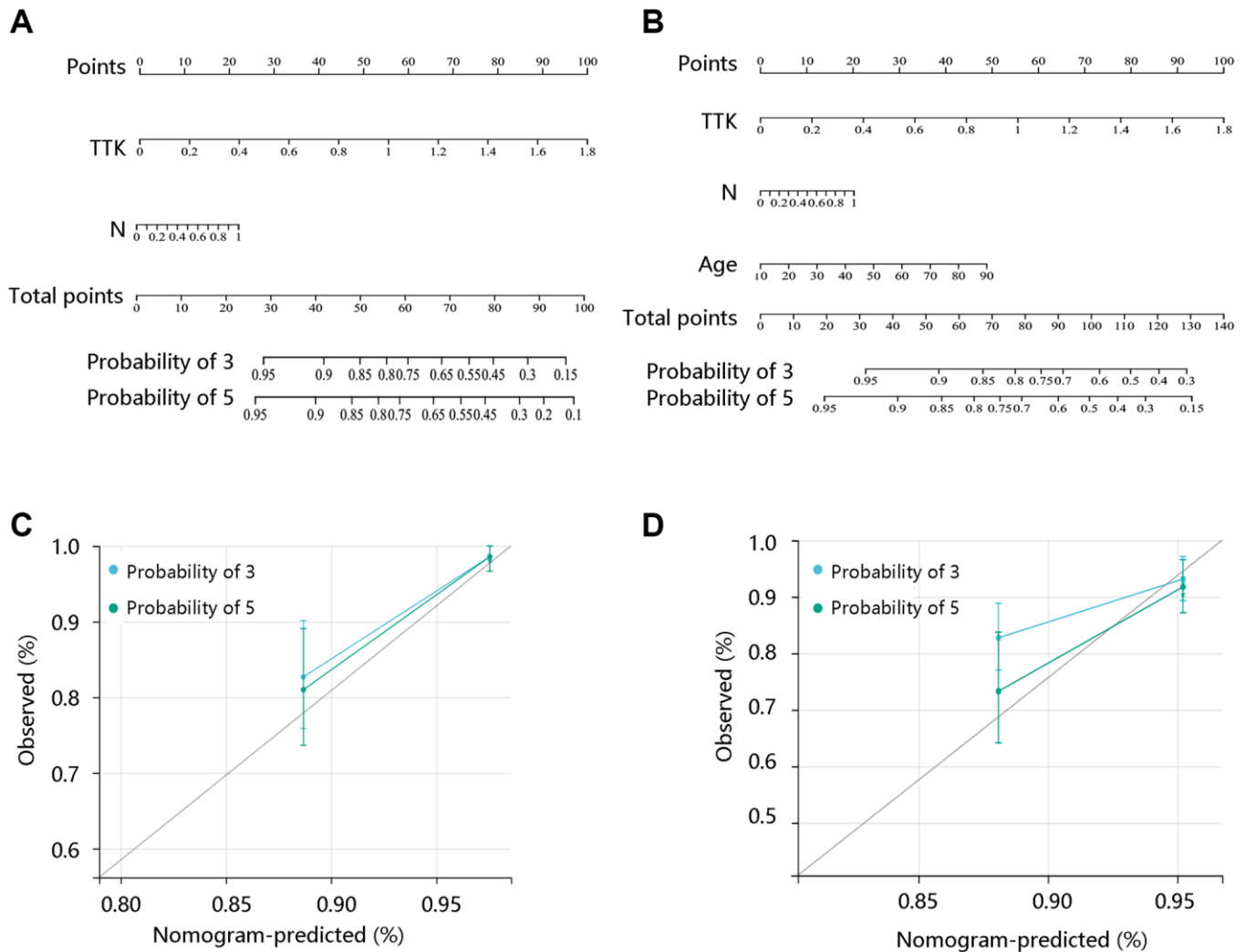


Figure 3. Construction and evaluation of nomogram models. Nomogram model construction by integrating the independent predictors for (A) DFI and (B) PFI. Evaluation of the nomogram models based on the (C) DFI and (D) PFI.

was significantly inhibited upon TTK knockdown. Besides, the migration of TPC1 and BCPAP cells was notably reduced once TTK was knocked down (Figure 7B). Then, the expressions of metastasis-related proteins MMP2, Snail, and Twist1 were examined. After TTK knockdown, the expressions of these proteins were downregulated (Figure 7C). These data indicated that TTK might be involved in PTC

metastasis. Epithelial-mesenchymal transition (EMT) participates in cancer cell invasion and migration. To confirm whether TTK accelerates PTC cell invasion and migration via EMT, we evaluated the expression of “EMT master genes”. Upon TTK-knockdown, two PTC cells exhibited increased E-cadherin expression and decreased M-cadherin and Vimentin expressions (Figure 7D). Therefore, TTK might modulate cell

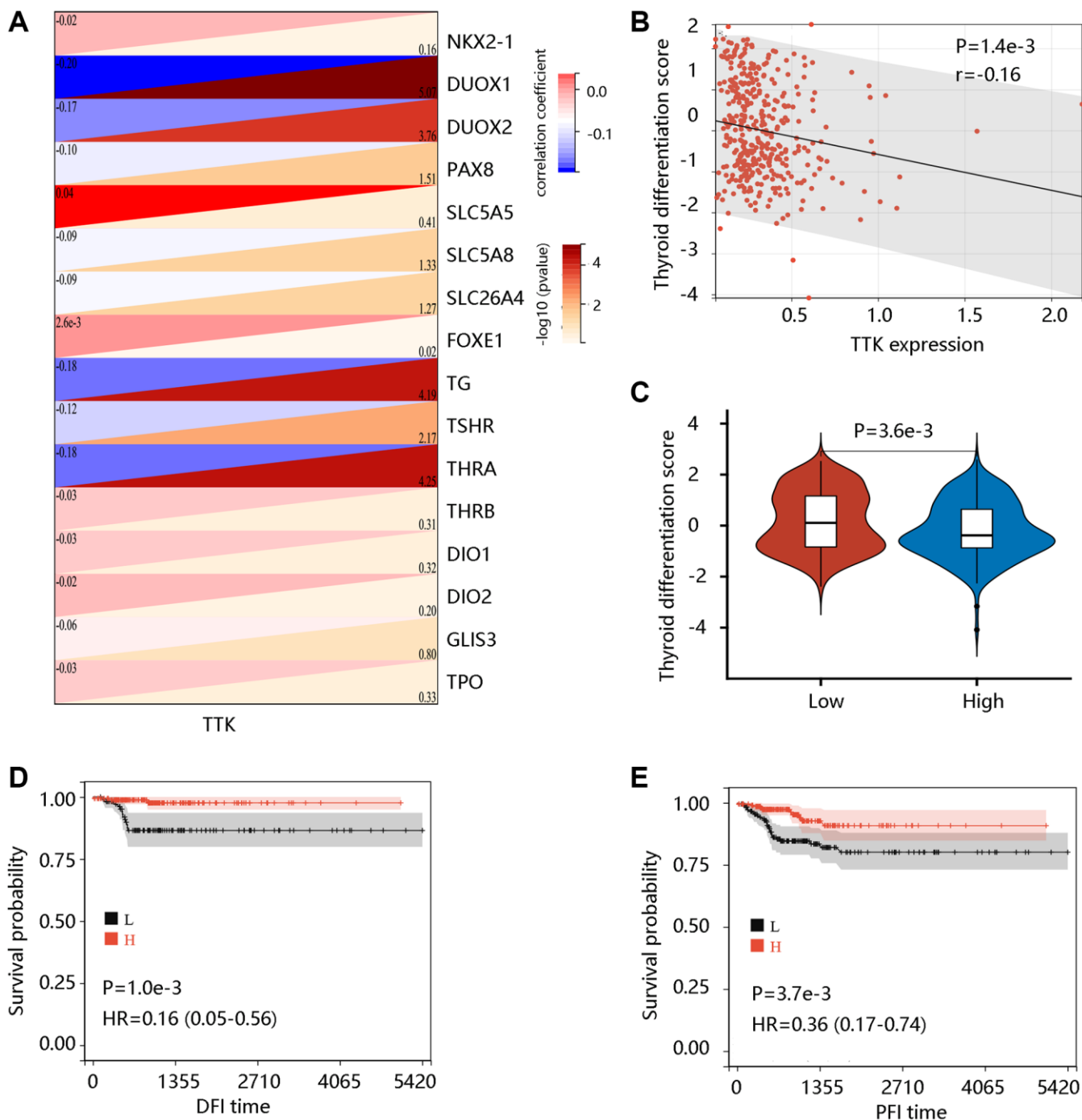


Figure 4. The value of TTK in PTC dedifferentiation. (A) Significant association of TTK with 16 thyroid-specific genes. (B) The significant negative correlation between TTK and thyroid differentiation score (TDS). (C) Higher TDS in low TTK expression group. Patients with high TDS had favorable (D) DFI and (E) PFI.

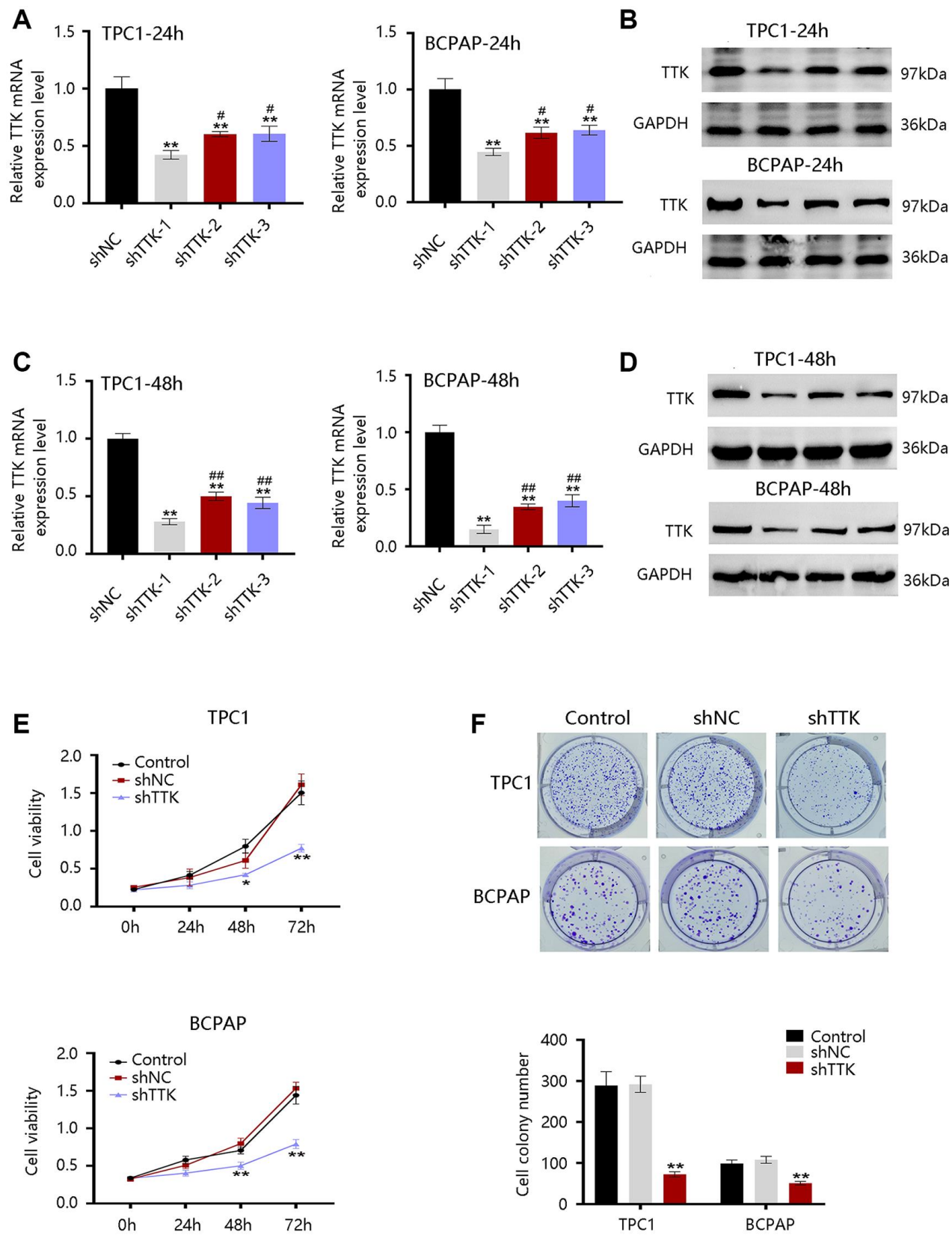


Figure 5. Effect of TTK on PTC cell growth. TTK knockdown efficiency of cells transfected with scrambled shRNA (shNC) or shRNAs against TTK (shTTK) for (A, B) 24 h and (C, D) 48 h in TPC1 and BCPAP cells. (E) The viability of TPC1 and BCPAP cells following TTK knockdown. (F) Representative images (up) and quantification (down) of colony formation assays of two cells. Compared with shNC, * $P < 0.05$, ** $P < 0.01$; compared with shTTK-1, # $P < 0.05$, ## $P < 0.01$.

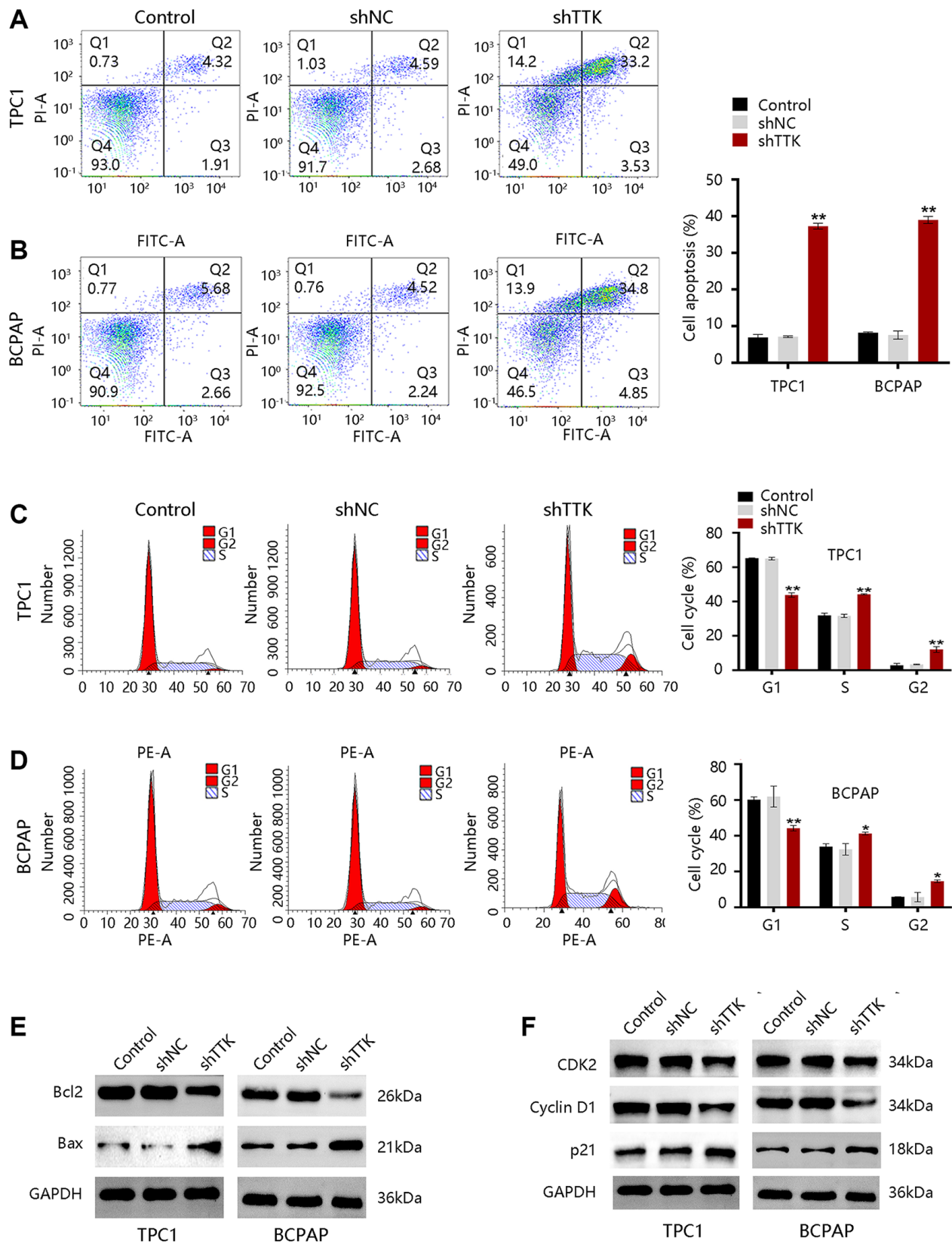


Figure 6. TTK inhibits cell apoptosis and accelerates cell cycle progression in TPC1 and BCPAP cells. (A, B) Results of cell apoptosis numbers (left) and cell apoptosis ratio (right). (C, D) Cell cycle results of peak diagrams (left) and cell distribution in different phases (right). Western blot for (E) apoptosis-related proteins and (F) cell cycle-related proteins in TTK-knockdown TPC1 and BCPAP cells. Compared with shNC, * $P < 0.05$, ** $P < 0.01$.

invasion and migration by accelerating the EMT process and it might be involved in PTC metastasis.

TTK activates the cell adhesion molecules (CAM) pathway

To explore the potential signaling pathways regulated by TTK, we identified the DEGs between TTK-H and

TTK-L (Figure 8A). We obtained 600 significant DEGs for analyzing the biological processes. As presented in Figure 8B, they mainly participated in the small molecule metabolic process, lipid metabolic process, and fatty acid metabolic process, which is essential in cancer cell migration and invasion. To meet the energy demands of cytoskeletal activity during migration, cells transport metabolic proteins and concentrate energy

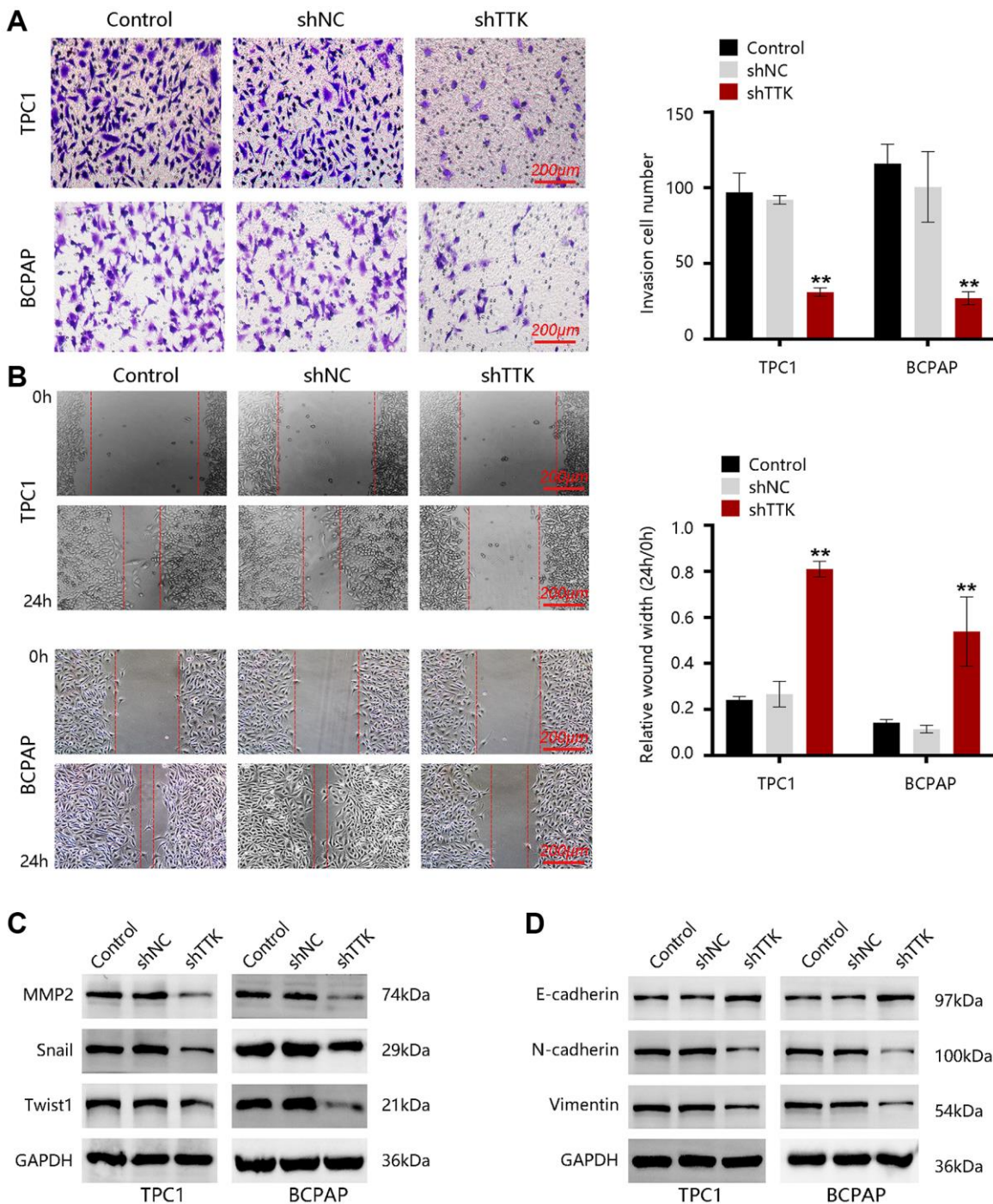


Figure 7. TTK promotes PTC cell invasion and migration. (A) The invasion of TPC1 and BCPAP cells transfected with shNC or shTTK and control for 24 h was measured by transwell invasion assay. (B) The migration of two PTC cells was assessed by wound-healing assay. Western blot for (C) metastasis-related proteins and (D) EMT marker genes in TTK-knockdown TPC1 and BCPAP cells. Compared with shNC, ** $P < 0.01$.

production to sites of high energy demand [27]. Subsequently, we performed GSEA and observed that the apoptosis, Toll-like receptor signaling pathway, natural killer cell-mediated cytotoxicity, cell cycle, and CAM were enriched in the TTK-H (Figure 8C).

Due to the potential value of TTK in metastasis, core proteins in the CAM signaling pathway were detected through western blotting. In the formation of metastasis, CAM plays a critical role in the adhesion of tumor cells to the endothelium. The protein expression of ICAM1, VCAM1, and MMP9 was decreased in TTK-downregulated TPC1 and BCPAP cells (Figure 8D). These findings suggested that TTK might promote PTC

malignancy, especially its metastasis via activating the CAM signaling pathway.

TTK was significantly associated with immune cell infiltration

To determine TTK involvement in the tumor immune microenvironment, we assessed the immune cell infiltrates using the ESTIMATE algorithm. A notable positive connection of TTK with immune- and stromal-scores was observed ($P < 0.05$) (Figure 9A). TIMER and xCELL algorithms confirmed that dendritic cells, T cell CD8, T cell CD4, and B cell were significantly linked to TTK (Figure 9B, 9C). The above findings

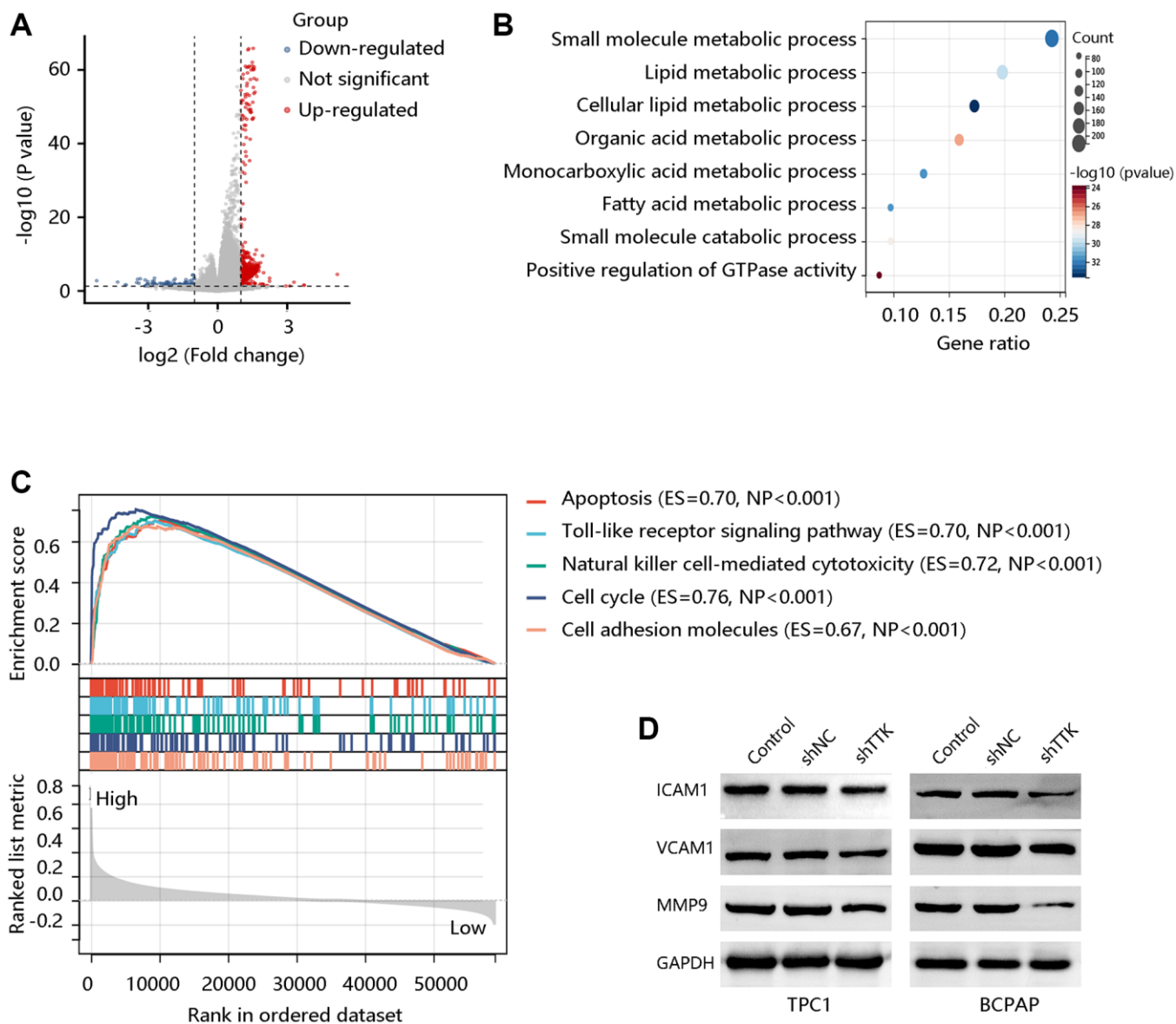


Figure 8. TTK activates the cell adhesion molecules (CAM) pathway. (A) The volcano plot shows differentially expressed genes (DEGs). (B) The biological processes of the significant DEGs. (C) Top five pathways enriched in high TTK expression group. (D) Western blot for the proteins in the CAM pathway.

PTC remains elucidated. Our study demonstrated high TTK expression in PTC and it had a certain value in predicting the DFI and PFI status in PTC. Besides, TTK overexpression independently predicted PTC prognosis

and was notably related to PTC dedifferentiation. TTK participated in PTC cell proliferation, apoptosis, cell cycle, migration, and invasion. These results suggested the potential clinical value of TTK in PTC.

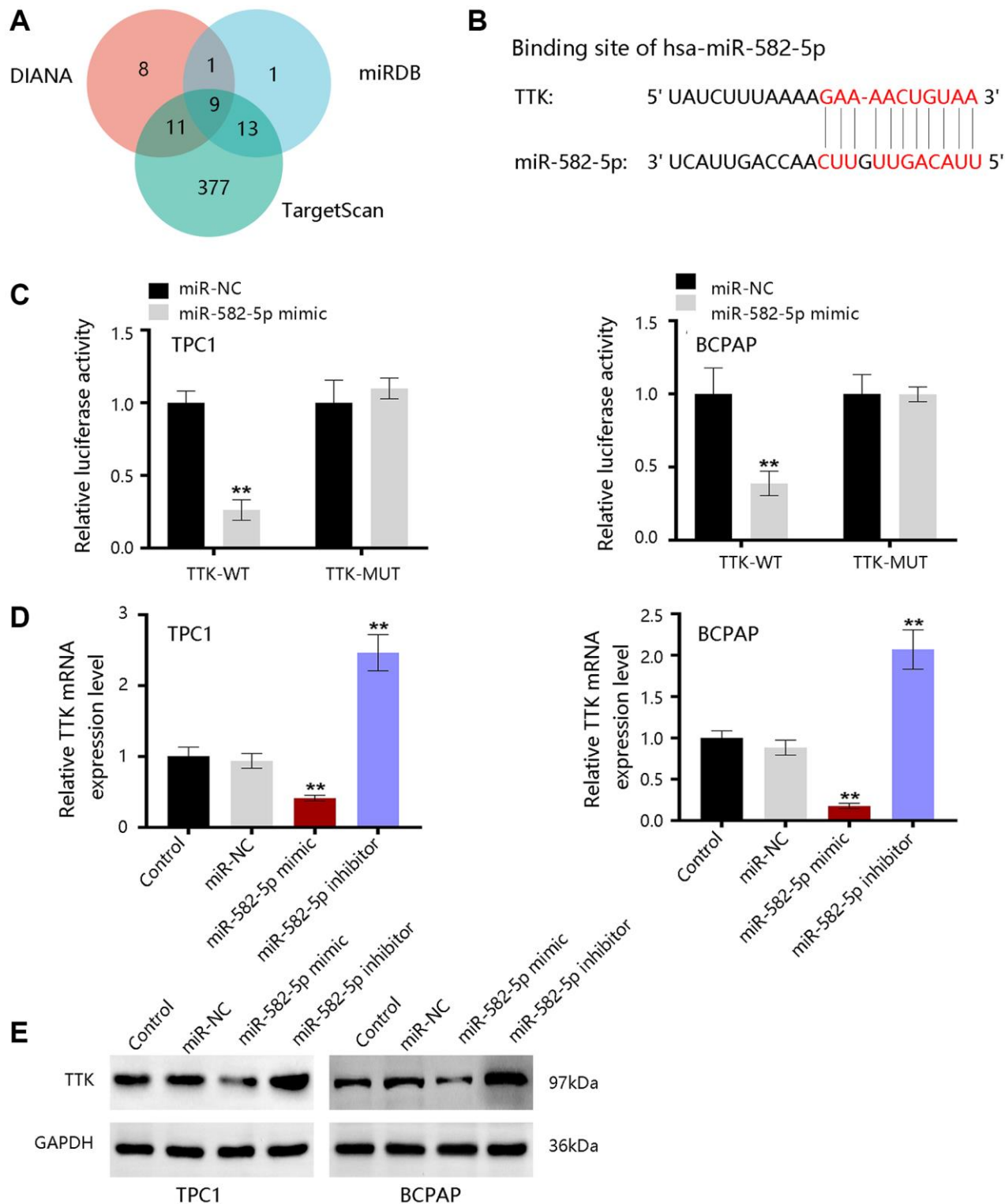


Figure 10. The upstream miRNAs of TTK. (A) Nine consistent miRNAs in three databases. (B) The binding site of miR-582-5p and TTK. (C) Validation of the binding site in TPC1 and BCPAP cells. (D) qRT-PCR and (E) western blot results for detecting expression change of TTK upon treatment of miR-582-5p mimics and inhibitors in PTC cells. Compared with miR-NC, $**P < 0.01$.

TTK plays a regulatory role in cancer cell proliferation, cell cycle, and apoptosis. Knockdown of TTK inhibited proliferation and increased apoptosis of gastric cancer cells through the Akt-mTOR pathway [31]. TTK depletion inhibited ovarian cancer cell proliferation by disturbing cell cycle progression [32]. In our study, PTC cell proliferation was suppressed, apoptosis was increased and the cell cycle was arrested after TTK was knockdown. The SAC is a conserved mitotic checkpoint that ensures accurate chromosome segregation during

mitosis [33]. The inactivation of SAC in cancer leads to unequal segregation of chromosomes during mitosis, resulting in aberrant chromosomal numbers and cellular aneuploidy, hence enhancing chromosomal instability and the frequency of mitotic defects [34]. The protein kinase TTK is required for SAC activation [35]. Through Knl1, Bub1, and Mad1 phosphorylation sequentially, TTK can promote checkpoint activation and recruit checkpoint proteins to kinetochores in mitosis progress to ensure error-free chromosome

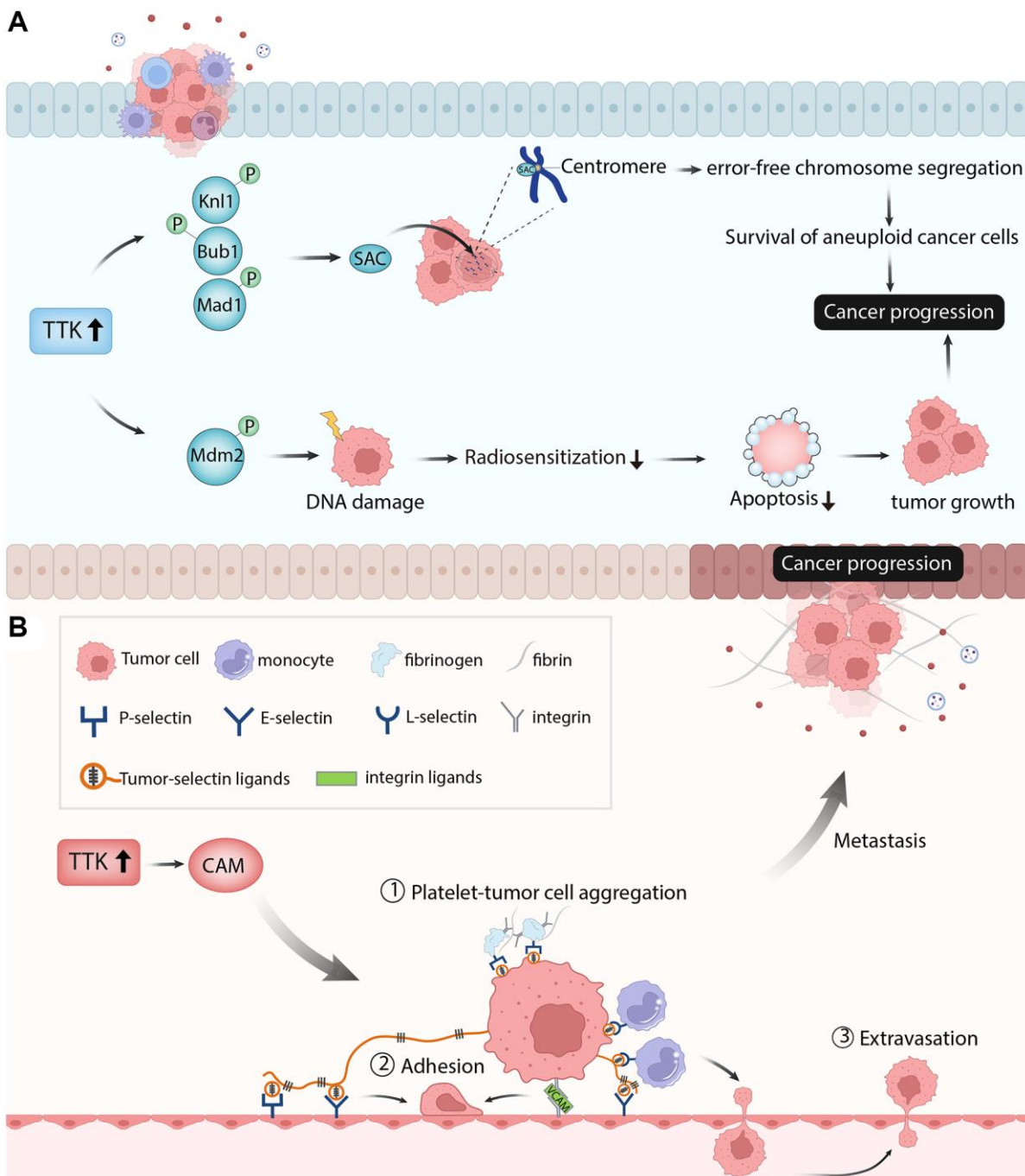


Figure 11. The diagram showed the possible mechanism of TTK involved in papillary thyroid cancer. (A) TTK was essential for tumor cell growth in the aspects of cell proliferation, cell cycle, and cell apoptosis. (B) TTK was related to cancer cell metastasis.

segregation [36]. Elevated levels of TTK allow the survival of aneuploidy cancer cells and its overexpression has been observed in multiple cancers. TTK knockdown in glioblastoma and colorectal cancer cell lines reduced cell viability, led to abnormal cell progression and increased apoptosis [29, 37]. Similarly, the depletion of TTK decreased colonic survival and increased apoptosis in the pancreatic ductal adenocarcinoma cell line [14]. Therefore, the authors speculated that TTK overexpression might activate SAC through phosphorylating the substrates to promote cancer cell growth. In addition to the regulation of mitosis, TTK also facilitates DNA damage through phosphorylating Mdm2 [38]. DNA damage reduced radiosensitization and decreased cancer cell death, promoting cancer progression [39]. These findings revealed that TTK was essential for tumor cell growth in the aspects of proliferation, cycle, and apoptosis (Figure 11A).

Subsequently, we investigated the role of TTK in PTC cell migration and invasion using wound-healing and transwell assays. The migratory and invasive capacities of TPC1 and BCPAP were inhibited upon TTK knockdown. For validation, we detected the expression of metastasis-related proteins and “EMT master genes”, revealing that TTK might modulate cell migration and invasion through accelerating EMT in PTC cell lines and it might be related to PTC metastasis.

Next, we performed the enrichment analysis of the significant DEGs and found that they were mainly involved in metabolism-related processes, which is essential in cancer cell migration and invasion. The GSEA result showed that TTK mainly participated in apoptosis, Toll-like receptor signaling pathway, natural killer cell-mediated cytotoxicity, cell cycle, and cell adhesion molecules. Cell adhesion molecules include selections, cadherins, integrins, and others [40]. These molecules directly affect immune invasion and metastasis by mediating interactions with other cells and the extracellular matrix in the microenvironment [41]. Through fibrin and fibrinogen, P-selectin and integrins mediate the formation of Platelet-tumor cell aggregates. P- and E-selectins mediate the adhesion of tumor cells to the endothelium, while integrin and its interaction with VCAM-1 on tumor cells promote firm adhesion. Monocytes lead to tumor cell extravasation by facilitating tumor cell-endothelial interactions. This process depends on the conjugation of E-selectin and integrin [42]. Thus, the authors speculated that TTK might accelerate PTC cell metastasis by regulating the cell adhesion molecules pathway (Figure 11B). Due to the vital role of immune cells in tumor progression and metastasis, we performed an immune cell infiltration analysis and found that TTK was significantly

correlated with several immune cells. The authors speculated that TTK might promote PTC development by influencing immune cell infiltration.

As short and highly conserved noncoding RNAs, miRNAs negatively regulate gene expression to modulate abundant biological processes. This study showed that miR-582-5p was an upstream regulator of TTK [43, 44]. Through its regulation of MTC proto-oncogene, aggressive phenotype would be suppressed in esophageal squamous cancer cells by miR-182 [45]. MiR-936 suppressed glioma progression by modulating ERBB4 [46]. Thus, the authors speculated that miR-582-5p might promote PTC progression by negatively regulating TTK expression.

For strengths, our study is novel in study design, which combines bioinformatics approaches with experiment verification. This is the first comprehensive research that systemically investigates the clinical significance of TTK in PTC and its overexpression promoting the PTC progression through accelerating cancer cell growth and metastasis. Moreover, this study reveals the possible mechanism of TTK involved in PTC. However, how the miR-582-5p regulates TTK expression to promote the PTC progression requires further investigation *in vitro*. The data from more independent cohorts will be applied for further analysis to validate the clinical value of TTK in PTC prognosis. The role of TTK in PTC dedifferentiation will be confirmed using *in vitro* experiments in the future.

In conclusion, TTK might be a potent regulator for tumor progression by the efficient bioinformatics approaches and validated by the *in vitro* experiments. Besides, TTK was significantly related to PTC dedifferentiation and immune cell infiltration. Finally, TTK expression can be modulated by miR-182-5p. These new findings indicated that TTK might be a potential biomarker and therapeutic target for PTC.

Abbreviations

TTK: threonine tyrosine kinase; PTC: papillary thyroid cancer; TDS: thyroid differentiation score; THCA: thyroid cancer; SAC: spindle assembly checkpoint; GSEA: gene set enrichment analysis; ROC: receiver operating characteristic; DFI: disease-free interval; DSS: disease-specific survival; OS: overall survival; PFI: progression-free interval; DEGs: differentially expressed genes; EMT: epithelial-mesenchymal transition.

AUTHOR CONTRIBUTIONS

Jun-Jie Ma contributed to the conception and design. Jun-Jie Ma and Cheng Xiang contributed to the

collection and assembly of data. Jun-Jie Ma and Jian-Wei Wang analyzed and interpreted the data. Jun-Jie Ma and Jian-Wei Wang performed the experiments mentioned in the paper. All authors wrote and approved the final manuscript.

CONFLICTS OF INTEREST

The authors declare no conflicts of interest related to this study.

FUNDING

This study was supported by The Second Affiliated Hospital of Zhejiang University School of Medicine.

REFERENCES

1. Seib CD, Sosa JA. Evolving Understanding of the Epidemiology of Thyroid Cancer. *Endocrinol Metab Clin North Am*. 2019; 48:23–35. <https://doi.org/10.1016/j.ecl.2018.10.002> PMID:[30717905](https://pubmed.ncbi.nlm.nih.gov/30717905/)
2. Sung H, Ferlay J, Siegel RL, Laversanne M, Soerjomataram I, Jemal A, Bray F. Global Cancer Statistics 2020: GLOBOCAN Estimates of Incidence and Mortality Worldwide for 36 Cancers in 185 Countries. *CA Cancer J Clin*. 2021; 71:209–49. <https://doi.org/10.3322/caac.21660> PMID:[33538338](https://pubmed.ncbi.nlm.nih.gov/33538338/)
3. Xie L, Wang S, Qian Y, Jia S, Wang J, Li L, Zhang W, Yu H, Bao P, Qian B. Increasing Gap Between Thyroid Cancer Incidence and Mortality in Urban Shanghai, China: An Analysis Spanning 43 Years. *Endocr Pract*. 2021; 27:1100–7. <https://doi.org/10.1016/j.eprac.2021.06.002> PMID:[34119680](https://pubmed.ncbi.nlm.nih.gov/34119680/)
4. Schwaiger K, Koeninger F, Wimbauer J, Heinrich K, Gala-Kokalj A, Wechselberger G. Occult papillary thyroid cancer presenting as cystic metastasis of the lateral neck: A case report. *Medicine (Baltimore)*. 2019; 98:e16659. <https://doi.org/10.1097/MD.00000000000016659> PMID:[31348321](https://pubmed.ncbi.nlm.nih.gov/31348321/)
5. Papaioannou M, Chorti AG, Chatzikyriakidou A, Giannoulis K, Bakkar S, Papavramidis TS. MicroRNAs in Papillary Thyroid Cancer: What Is New in Diagnosis and Treatment. *Front Oncol*. 2022; 11:755097. <https://doi.org/10.3389/fonc.2021.755097> PMID:[35186709](https://pubmed.ncbi.nlm.nih.gov/35186709/)
6. Na DG, Baek JH, Jung SL, Kim JH, Sung JY, Kim KS, Lee JH, Shin JH, Choi YJ, Ha EJ, Lim HK, Kim SJ, Hahn SY, et al, and Korean Society of Thyroid Radiology (KSThR) and Korean Society of Radiology. Core Needle Biopsy of the Thyroid: 2016 Consensus Statement and Recommendations from Korean Society of Thyroid Radiology. *Korean J Radiol*. 2017; 18:217–37. <https://doi.org/10.3348/kjr.2017.18.1.217> PMID:[28096731](https://pubmed.ncbi.nlm.nih.gov/28096731/)
7. Ahn SH, Park SY, Choi SI. Comparison of Consecutive Results from Fine Needle Aspiration and Core Needle Biopsy in Thyroid Nodules. *Endocr Pathol*. 2017; 28:332–8. <https://doi.org/10.1007/s12022-017-9496-1> PMID:[28748505](https://pubmed.ncbi.nlm.nih.gov/28748505/)
8. Nixon IJ, Simo R, Newbold K, Rinaldo A, Suarez C, Kowalski LP, Silver C, Shah JP, Ferlito A. Management of Invasive Differentiated Thyroid Cancer. *Thyroid*. 2016; 26:1156–66. <https://doi.org/10.1089/thy.2016.0064> PMID:[27480110](https://pubmed.ncbi.nlm.nih.gov/27480110/)
9. Ito Y, Miyauchi A, Kihara M, Fukushima M, Higashiyama T, Miya A. Overall Survival of Papillary Thyroid Carcinoma Patients: A Single-Institution Long-Term Follow-Up of 5897 Patients. *World J Surg*. 2018; 42:615–22. <https://doi.org/10.1007/s00268-018-4479-z> PMID:[29349484](https://pubmed.ncbi.nlm.nih.gov/29349484/)
10. Prete A, Borges de Souza P, Censi S, Muzza M, Nucci N, Sponziello M. Update on Fundamental Mechanisms of Thyroid Cancer. *Front Endocrinol (Lausanne)*. 2020; 11:102. <https://doi.org/10.3389/fendo.2020.00102> PMID:[32231639](https://pubmed.ncbi.nlm.nih.gov/32231639/)
11. Yakushina VD, Lerner LV, Lavrov AV. Gene Fusions in Thyroid Cancer. *Thyroid*. 2018; 28:158–67. <https://doi.org/10.1089/thy.2017.0318> PMID:[29281951](https://pubmed.ncbi.nlm.nih.gov/29281951/)
12. Gugnoni M, Manicardi V, Torricelli F, Sauta E, Bellazzi R, Manzotti G, Vitale E, de Biase D, Piana S, Ciarrocchi A. Linc00941 Is a Novel Transforming Growth Factor β Target That Primes Papillary Thyroid Cancer Metastatic Behavior by Regulating the Expression of Cadherin 6. *Thyroid*. 2021; 31:247–63. <https://doi.org/10.1089/thy.2020.0001> PMID:[32495722](https://pubmed.ncbi.nlm.nih.gov/32495722/)
13. Cabanillas ME, Ryder M, Jimenez C. Targeted Therapy for Advanced Thyroid Cancer: Kinase Inhibitors and Beyond. *Endocr Rev*. 2019; 40:1573–604. <https://doi.org/10.1210/er.2019-00007> PMID:[31322645](https://pubmed.ncbi.nlm.nih.gov/31322645/)
14. Kaistha BP, Honstein T, Müller V, Bielak S, Sauer M, Kreider R, Fassan M, Scarpa A, Schmees C, Volkmer H, Gress TM, Buchholz M. Key role of dual specificity kinase TTK in proliferation and survival of pancreatic cancer cells. *Br J Cancer*. 2014; 111:1780–7.

- <https://doi.org/10.1038/bjc.2014.460>
PMID:[25137017](https://pubmed.ncbi.nlm.nih.gov/25137017/)
15. Lara-Gonzalez P, Westhorpe FG, Taylor SS. The spindle assembly checkpoint. *Curr Biol.* 2012; 22:R966–80.
<https://doi.org/10.1016/j.cub.2012.10.006>
PMID:[23174302](https://pubmed.ncbi.nlm.nih.gov/23174302/)
16. Musacchio A. The Molecular Biology of Spindle Assembly Checkpoint Signaling Dynamics. *Curr Biol.* 2015; 25:R1002–18.
<https://doi.org/10.1016/j.cub.2015.08.051>
PMID:[26485365](https://pubmed.ncbi.nlm.nih.gov/26485365/)
17. Thu KL, Silvester J, Elliott MJ, Ba-Alawi W, Duncan MH, Elia AC, Mer AS, Smirnov P, Safikhani Z, Haibe-Kains B, Mak TW, Cescon DW. Disruption of the anaphase-promoting complex confers resistance to TTK inhibitors in triple-negative breast cancer. *Proc Natl Acad Sci U S A.* 2018; 115:E1570–7.
<https://doi.org/10.1073/pnas.1719577115>
PMID:[29378962](https://pubmed.ncbi.nlm.nih.gov/29378962/)
18. Faisal A, Mak GWY, Gurden MD, Xavier CPR, Anderhub SJ, Innocenti P, Westwood IM, Naud S, Hayes A, Box G, Valenti MR, De Haven Brandon AK, O'Fee L, et al. Characterisation of CCT271850, a selective, oral and potent MPS1 inhibitor, used to directly measure in vivo MPS1 inhibition vs therapeutic efficacy. *Br J Cancer.* 2017; 116:1166–76.
<https://doi.org/10.1038/bjc.2017.75>
PMID:[28334731](https://pubmed.ncbi.nlm.nih.gov/28334731/)
19. Wang J, Xie Y, Bai X, Wang N, Yu H, Deng Z, Lian M, Yu S, Liu H, Xie W, Wang M. Targeting dual specificity protein kinase TTK attenuates tumorigenesis of glioblastoma. *Oncotarget.* 2017; 9:3081–8.
<https://doi.org/10.18632/oncotarget.23152>
PMID:[29423030](https://pubmed.ncbi.nlm.nih.gov/29423030/)
20. Zhang YJ, Oh JL, Whitman GJ, Iyengar P, Yu TK, Tereffe W, Woodward WA, Perkins G, Buchholz TA, Strom EA. Clinically apparent internal mammary nodal metastasis in patients with advanced breast cancer: incidence and local control. *Int J Radiat Oncol Biol Phys.* 2010; 77:1113–9.
<https://doi.org/10.1016/j.ijrobp.2009.06.081>
PMID:[20004535](https://pubmed.ncbi.nlm.nih.gov/20004535/)
21. Zhang Q, Xia T, Qi C, Du J, Ye C. High expression of S100A2 predicts poor prognosis in patients with endometrial carcinoma. *BMC Cancer.* 2022; 22:77.
<https://doi.org/10.1186/s12885-022-09180-5>
PMID:[35042454](https://pubmed.ncbi.nlm.nih.gov/35042454/)
22. Sunakorn B, Bamrungtrakul T. A comparative study of Thai liquid and freeze-dried BCG vaccine with Japanese freeze-dried BCG vaccine. *J Med Assoc Thai.* 1970; 53:836–42.
PMID:[5532416](https://pubmed.ncbi.nlm.nih.gov/5532416/)
23. Bhatia S, Nguyen D, Darragh LB, Van Court B, Sharma J, Knitz MW, Piper M, Bukkapatnam S, Gadwa J, Bickett TE, Bhuvane S, Corbo S, Wu B, et al. EphB4 and ephrinB2 act in opposition in the head and neck tumor microenvironment. *Nat Commun.* 2022; 13:3535.
<https://doi.org/10.1038/s41467-022-31124-7>
PMID:[35725568](https://pubmed.ncbi.nlm.nih.gov/35725568/)
24. Ke KJ, Wang CY, Li P, Huang XW, Zhang SL, Li X, Cui XF. Hsa_circ_001193 regulates proliferation and apoptosis of nasopharyngeal carcinoma cells through targeting mir-496. *Eur Rev Med Pharmacol Sci.* 2020; 24:3069–76.
https://doi.org/10.26355/eurrev_202003_20671
PMID:[32271424](https://pubmed.ncbi.nlm.nih.gov/32271424/)
25. Pan RH, Zhang X, Chen ZP, Liu YJ. Arachidonate lipoxygenases 5 is a novel prognostic biomarker and correlates with high tumor immune infiltration in low-grade glioma. *Front Genet.* 2023; 14:1027690.
<https://doi.org/10.3389/fgene.2023.1027690>
PMID:[36777735](https://pubmed.ncbi.nlm.nih.gov/36777735/)
26. Lu N, Ren L. TTK (threonine tyrosine kinase) regulates the malignant behaviors of cancer cells and is regulated by microRNA-582-5p in ovarian cancer. *Bioengineered.* 2021; 12:5759–68.
<https://doi.org/10.1080/21655979.2021.1968778>
PMID:[34516342](https://pubmed.ncbi.nlm.nih.gov/34516342/)
27. Kelley LC, Chi Q, Cáceres R, Hastie E, Schindler AJ, Jiang Y, Matus DQ, Plastino J, Sherwood DR. Adaptive F-Actin Polymerization and Localized ATP Production Drive Basement Membrane Invasion in the Absence of MMPs. *Dev Cell.* 2019; 48:313–28.e8.
<https://doi.org/10.1016/j.devcel.2018.12.018>
PMID:[30686527](https://pubmed.ncbi.nlm.nih.gov/30686527/)
28. Ling Y, Zhang X, Bai Y, Li P, Wei C, Song T, Zheng Z, Guan K, Zhang Y, Zhang B, Liu X, Ma RZ, Cao C, et al. Overexpression of Mps1 in colon cancer cells attenuates the spindle assembly checkpoint and increases aneuploidy. *Biochem Biophys Res Commun.* 2014; 450:1690–5.
<https://doi.org/10.1016/j.bbrc.2014.07.071>
PMID:[25063032](https://pubmed.ncbi.nlm.nih.gov/25063032/)
29. Wengner AM, Siemeister G, Koppitz M, Schulze V, Kosemund D, Klar U, Stoeckigt D, Neuhaus R, Lienau P, Bader B, Prechtel S, Raschke M, Frisk AL, et al. Novel Mps1 Kinase Inhibitors with Potent Antitumor Activity. *Mol Cancer Ther.* 2016; 15:583–92.
<https://doi.org/10.1158/1535-7163.MCT-15-0500>
PMID:[26832791](https://pubmed.ncbi.nlm.nih.gov/26832791/)
30. Maachani UB, Kramp T, Hanson R, Zhao S, Celiku O, Shankavaram U, Colombo R, Caplen NJ, Camphausen K, Tandle A. Targeting MPS1 Enhances Radio-sensitization of Human Glioblastoma by Modulating

- DNA Repair Proteins. *Mol Cancer Res.* 2015; 13:852–62.
<https://doi.org/10.1158/1541-7786.MCR-14-0462-T>
PMID:[25722303](https://pubmed.ncbi.nlm.nih.gov/25722303/)
31. Huang H, Yang Y, Zhang W, Liu X, Yang G. TTK regulates proliferation and apoptosis of gastric cancer cells through the Akt-mTOR pathway. *FEBS Open Bio.* 2020; 10:1542–9.
<https://doi.org/10.1002/2211-5463.12909>
PMID:[32530571](https://pubmed.ncbi.nlm.nih.gov/32530571/)
32. Qi G, Ma H, Li Y, Peng J, Chen J, Kong B. TTK inhibition increases cisplatin sensitivity in high-grade serous ovarian carcinoma through the mTOR/autophagy pathway. *Cell Death Dis.* 2021; 12:1135.
<https://doi.org/10.1038/s41419-021-04429-6>
PMID:[34876569](https://pubmed.ncbi.nlm.nih.gov/34876569/)
33. Stratford JK, Yan F, Hill RA, Major MB, Graves LM, Der CJ, Yeh JJ. Genetic and pharmacological inhibition of TTK impairs pancreatic cancer cell line growth by inducing lethal chromosomal instability. *PLoS One.* 2017; 12:e0174863.
<https://doi.org/10.1371/journal.pone.0174863>
PMID:[28380042](https://pubmed.ncbi.nlm.nih.gov/28380042/)
34. El-Karim EA, Hagos EG, Ghaleb AM, Yu B, Yang VW. Krüppel-like factor 4 regulates genetic stability in mouse embryonic fibroblasts. *Mol Cancer.* 2013; 12:89.
<https://doi.org/10.1186/1476-4598-12-89>
PMID:[23919723](https://pubmed.ncbi.nlm.nih.gov/23919723/)
35. Wu Q, Li Z, Huang Y, Qian D, Chen M, Xiao W, Wang B. Oxidative Stress Delays Prometaphase/Metaphase of the First Cleavage in Mouse Zygotes via the MAD2L1-Mediated Spindle Assembly Checkpoint. *Oxid Med Cell Longev.* 2017; 2017:2103190.
<https://doi.org/10.1155/2017/2103190>
PMID:[29147457](https://pubmed.ncbi.nlm.nih.gov/29147457/)
36. Ji Z, Gao H, Jia L, Li B, Yu H. A sequential multi-target Mps1 phosphorylation cascade promotes spindle checkpoint signaling. *Elife.* 2017; 6:e22513.
<https://doi.org/10.7554/eLife.22513>
PMID:[28072388](https://pubmed.ncbi.nlm.nih.gov/28072388/)
37. Kwiatkowski N, Jelluma N, Filippakopoulos P, Soundararajan M, Manak MS, Kwon M, Choi HG, Sim T, Deveraux QL, Rottmann S, Pellman D, Shah JV, Kops GJ, et al. Small-molecule kinase inhibitors provide insight into Mps1 cell cycle function. *Nat Chem Biol.* 2010; 6:359–68.
<https://doi.org/10.1038/nchembio.345>
PMID:[20383151](https://pubmed.ncbi.nlm.nih.gov/20383151/)
38. Wang ZX, Ren SC, Ren J. Phosphotyrosine picked threonine kinase stimulates proliferation of human osteosarcoma cells *in vitro* and *in vivo*. *Arch Med Sci.* 2021; 18:775–85.
<https://doi.org/10.5114/aoms/115135>
PMID:[35591845](https://pubmed.ncbi.nlm.nih.gov/35591845/)
39. Chandler BC, Moubadder L, Ritter CL, Liu M, Cameron M, Wilder-Romans K, Zhang A, Pesch AM, Michmerhuizen AR, Hirsh N, Androsiglio M, Ward T, Olsen E, et al. TTK inhibition radiosensitizes basal-like breast cancer through impaired homologous recombination. *J Clin Invest.* 2020; 130:958–73.
<https://doi.org/10.1172/JCI130435>
PMID:[31961339](https://pubmed.ncbi.nlm.nih.gov/31961339/)
40. Harjunpää H, Lloret Asens M, Guenther C, Fagerholm SC. Cell Adhesion Molecules and Their Roles and Regulation in the Immune and Tumor Microenvironment. *Front Immunol.* 2019; 10:1078.
<https://doi.org/10.3389/fimmu.2019.01078>
PMID:[31231358](https://pubmed.ncbi.nlm.nih.gov/31231358/)
41. Cooper J, Giancotti FG. Integrin Signaling in Cancer: Mechanotransduction, Stemness, Epithelial Plasticity, and Therapeutic Resistance. *Cancer Cell.* 2019; 35:347–67.
<https://doi.org/10.1016/j.ccell.2019.01.007>
PMID:[30889378](https://pubmed.ncbi.nlm.nih.gov/30889378/)
42. Läubli H, Borsig L. Altered Cell Adhesion and Glycosylation Promote Cancer Immune Suppression and Metastasis. *Front Immunol.* 2019; 10:2120.
<https://doi.org/10.3389/fimmu.2019.02120>
PMID:[31552050](https://pubmed.ncbi.nlm.nih.gov/31552050/)
43. Mishra S, Yadav T, Rani V. Exploring miRNA based approaches in cancer diagnostics and therapeutics. *Crit Rev Oncol Hematol.* 2016; 98:12–23.
<https://doi.org/10.1016/j.critrevonc.2015.10.003>
PMID:[26481951](https://pubmed.ncbi.nlm.nih.gov/26481951/)
44. Lu TX, Rothenberg ME. MicroRNA. *J Allergy Clin Immunol.* 2018; 141:1202–7.
<https://doi.org/10.1016/j.jaci.2017.08.034>
PMID:[29074454](https://pubmed.ncbi.nlm.nih.gov/29074454/)
45. Wang J, Zhu W, Tao G, Wang W. Circular RNA circ-LRP6 facilitates Myc-driven tumorigenesis in esophageal squamous cell cancer. *Bioengineered.* 2020; 11:932–8.
<https://doi.org/10.1080/21655979.2020.1809922>
PMID:[32867570](https://pubmed.ncbi.nlm.nih.gov/32867570/)
46. Zhou D, Lin X, Wang P, Yang Y, Zheng J, Zhou D. Circular RNA circ_0001162 promotes cell proliferation and invasion of glioma via the miR-936/ERBB4 axis. *Bioengineered.* 2021; 12:2106–18.
<https://doi.org/10.1080/21655979.2021.1932221>
PMID:[34057019](https://pubmed.ncbi.nlm.nih.gov/34057019/)